STRUCTURE AND PROPERTIES OF MELT-SPUN Al-Zr-Ti ALLOYS I. COMPOSITION OF AS-MELT-SPUN RIBBONS

PŘEMYSL MÁLEK, PAVEL BARTUŠKA, JOSEF PLEŠTIL

The Al-Zr-Ti system has recently been suggested as a candidate for Al-based materials capable of retaining a high strength during a long term exposure to high temperatures up to 700 K. The Al-1.25at.%(Zr+Ti) alloys with a variable Zr : Ti ratio were rapidly solidified using the chill block melt spinning method. The homogeneity of the chemical composition was verified using the energy dispersive (EDX) and wave dispersive (WDA) X-ray analysis methods. The investigation of the phase composition of as-melt spun ribbons performed using the small angle X-ray scattering (SAXS) method revealed the presence of second-phase particles. In Zr-rich alloys, the fine second-phase particles were identified to be formed by the metastable $Al_3(Zr_xTi_{1-x})$ phase with the cubic $L1_2$ structure. The coarse particles present in the Ti-rich alloys were preferably constitutional particles in the spectrum of which Fe was found.

Key words: Al-based alloys for elevated temperatures, rapid solidification, chemical and phase composition, X-ray analysis

STRUKTURA A VLASTNOSTI SLITIN Al-Zr-Ti PŘIPRAVENÝCH METODOU „MELT SPINNING" I. SLOŽENÍ PÁSKŮ

Systém Al-Zr-Ti byl navržen jako jeden z kandidátů pro vývoj hliníkových slitin, které by byly schopny si uchovat vysokou pevnost během dlouhodobého pobytu za vysokých teplot (až do 700 K). Slitiny Al-1,25at.% (Zr+Ti) s proměnným poměrem Zr : Ti byly připraveny s vysokou rychlostí tuhnutí nástřikem taveniny na

RNDr. P. Málek, CSc., Department of Metal Physics, Charles University, Ke Karlovu 5, 12116 Prague 2, Czech Republic.

Ing. P. Bartuška, CSc., Institute of Physics, Academy of Sciences of the Czech Republic, Na Slovance 2, 18040 Prague 8, Czech Republic.

Ing. J. Pleštil, CSc., Institute of Macromolecular Chemistry, Academy of Sciences of the Czech Republic, Heyrovského nám. 1, 16000 Prague 6, Czech Republic.

rotující měděný válec. Homogenita chemického složení byla ověřována metodami energiově disperzní (EDX) a vlnově disperzní (WDA) analýzy rtg. záření. Studium fázového složení rychle ztuhlých pásků metodou nízkoúhlového rozptylu rtg. záření (SAXS) prokázalo přítomnost částic druhé fáze. Ve slitinách bohatých na Zr bylo zjištěno, že velmi jemné částice jsou tvořeny metastabilní fází $Al_3(Zr_xTi_{1-x})$ s kubickou strukturou typu $L1_2$. Velké částice přítomné ve slitinách bohatých na Ti byly interpretovány jako konstituční částice a v jejich spektru byla zjištěna přítomnost Fe.

1. Introduction

The substitution of high-strength Al-based alloys for Ti-based ones in elevated temperature applications (up to 700 K) is a challenging task of modern metallurgy. One of the ways how to solve this task is to design Al-based alloys with a high volume fraction of very small second-phase particles which do not dissolve at elevated temperatures and contribute to the high strength through a dispersion or precipitation strengthening. The strengthening effect of second-phase particles generally decreases with their increasing size. In order to retain a high strength at elevated temperatures, the particle coarsening has to be prevented. According to the theory of diffusion controlled ripening [1, 2] the coarsening rate decreases with decreasing diffusion rate of the particle-forming solute and with decreasing lattice mismatch between the strengthening phase and matrix.

Current age-hardenable aluminium alloys cannot be used for designing the materials for elevated temperature applications as any annealing at temperatures above about 423 K results in the coarsening or the dissolution of strengthening phases and, therefore, in a drop of strength. New compositions and producing methods must be sought. The suitable additives for elevated temperature Al-based alloys has to meet the following requirements:

– a capability to form intermetallic phases which have a low lattice mismatch to the Al-matrix,

– a low equilibrium solid solubility up to temperatures of 700 K in order to prevent the dissolution of strengthening phases,

– a low diffusivity in Al in order to slow down the diffusion controlled coarsening of strengthening phases particles.

Transition metals as Fe, Ni, Cr, Ti, V or Zr meet these requirements [3]. Zirconium has a special position among these additives. The equilibrium solid solubility of Zr in Al is very small and reaches its maximum of 0.28 wt.% at 934 K [4]. The diffusion rate of Zr in Al is the lowest among the above mentioned additives [5]. It forms the Al_3Zr intermetallic phase, the tetragonal DO_{23} structure of which has a low lattice mismatch to Al-matrix (about 2.9% [6]). The formation of this equilibrium phase is usually preceded by the formation of a metastable Al_3Zr phase with the cubic $L1_2$ structure which has even smaller lattice mismatch (about 0.7%

[7]). Therefore, the metastable Al_3Zr phase should be more resistant to coarsening and contribute more to the high strength at high temperatures than the equilibrium one.

Lattice mismatches of both modifications of the Al_3Zr phase may be modified by ternary additives as V, Hf or Ti [8, 9]. The atoms of these additives are believed to substitute for Zr atoms in the lattice of the strengthening phase and change slightly its lattice parameter. A suitable ratio between Zr and ternary atoms may reduce the lattice mismatch of the strengthening phase to zero which should result in a better structure and strength stability. An extensive study on the Al-Zr-V system confirmed this expectation. However, the formation of an additional $Al_{10}V$ phase especially at grain boundaries of the Al-matrix deteriorated the mechanical properties [10, 11]. The selection of Ti as the ternary additive should avoid this difficulty. The measurement of the coarsening rate in the Al-Zr-Ti alloy containing about 1 vol.% of the $Al_3(Zr_{0.75}Ti_{0.25})$ phase revealed the extraordinary stability of this alloy at 698 K [12].

Conventional ingot metallurgy processing route results in massive segregation and formation of coarse primary particles, and the desired structure with a homogeneous distribution of small second-phase particles cannot be formed. On the other hand, rapid solidification techniques with quenching rates up to 10^6 $K.s^{-1}$ successively extend the solid solubility limits, suppress the formation of primary particles, and homogenise and refine the solidified structure [13]. The desirable distribution of second-phase particles contributing to a high strength can be then formed through a decomposition of the supersaturated matrix during the subsequent annealing.

The Al-Zr-Ti system with a variable Zr and Ti content was chosen in our experiments, thin ribbons were prepared using the chill block melt spinning method and studied using numerous experimental methods. The experimental results are presented in four separate articles. The final objective of our investigation was to study the stability of the structure and mechanical properties of these ribbons during their long term exposure to elevated temperatures. As the structure inhomogeneity which is typical for as-melt-spun ribbons may significantly influence their properties, a great attention was paid to this aspect also in the Al-Zr-Ti system. The first part of our investigation deals with the homogeneity of the chemical and phase composition. The second part is devoted to the solidification microstructure and its influence on mechanical properties. The main aim of the third part is the investigation of phase transformations occurring during annealing at elevated temperatures and the last part correlates the microhardness values with the structure evolution at elevated temperatures.

2. Experimental material and procedure

The Al-Zr-Ti alloys with the equilibrium phase composition of Al-5vol.%

Table 1. Chemical composition of the Al-$Al_3(Zr_xTi_{1-x})$ alloys in wt.%

x	Nominal composition		EDX analysis chilled surface		EDX analysis free surface	
	Zr	Ti	Zr	Ti	Zr	Ti
1	4.1	–	4.0 ± 0.2	–	3.9 ± 0.5	–
0.75	3.1	0.55	3.1 ± 0.2	0.6 ± 0.1	3.1 ± 0.6	0.6 ± 0.1
0.5	2.1	1.1	2.1 ± 0.2	1.2 ± 0.1	2.3 ± 0.4	1.4 ± 0.1
0.25	1.0	1.65	1.0 ± 0.1	1.7 ± 0.1	0.9 ± 0.3	1.8 ± 0.1
0	–	2.2	–	2.3 ± 0.1	–	2.4 ± 0.2

$Al_3(Zr_xTi_{1-x})$ in a fully precipitated state were used in our experiments. The stoichiometric parameters $x = 1$, 0.75, 0.5, 0.25, and 0 were chosen. The nominal chemical compositions of these alloys are given in Table 1. The precastings prepared from 99.995% Al, Al-6wt.%Zr and Al-10wt.%Ti master alloys were remelted by the induction melting in a boron-nitride crucible and the melt was then ejected using argon gas pressure (5×10^4 Pa) onto a rotating copper wheel located in a chamber evacuated to 5×10^{-3} Pa. The melt spun ribbons of the thickness between 15 and 40 μm and the width between 1 and 2 mm were prepared.

The chemical composition was studied using the X-ray microanalyser JEOL Superprobe 733. The EDX analyses were performed both on the as-received chilled and free surfaces, metallographically processed transversal sections were analysed by the WDA technique. In order to control the homogeneity and possible directionality of the chemical composition the point analyses were carried out at different places along the longitudinal and transversal directions of ribbons.

The small angle X-ray scattering (SAXS) investigation of the ribbons was performed using a Kratky Camera equipped with a linear position sensitive detector. The measured scattering intensity was converted into the normalised intensity by means of a Lupolen standard.

The phase composition was studied using the X-ray diffraction analysis. The measurements were performed using Cu-Kα radiation in the diffractometer Siemens-Kristalloflex at room temperature with the scanning regime 0.02°/30 s. The Si reference powder was added to some samples as the X-ray peak position standard.

3. Experimental results

3.1 The chemical composition

The rates of solidification and cooling of the solidified material decrease with increasing distance from the contact (chilled) surface in the melt spinning process. This gradient may significantly influence the composition, the structure, and

physical properties and, therefore, both surfaces of the ribbons have to be investigated separately. Moreover, the thickness of melt-spun ribbons is variable (see the transversal section of the Al-Zr ribbon in Fig. 1) and the structure and properties of the melt spun material may be different at places with different ribbon thickness.

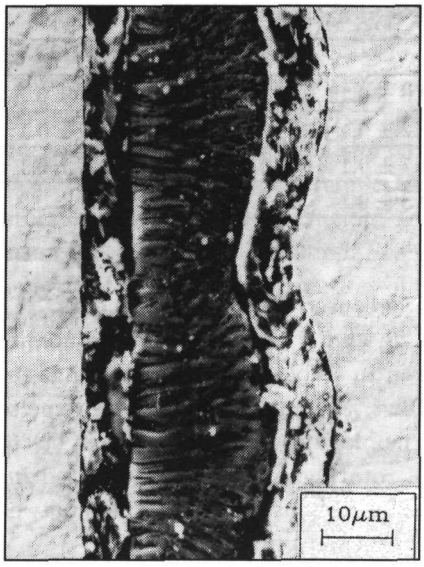

Fig. 1. The transversal section of the Al-Zr ribbon (covered by pure Ni), contact surface at the left, SEM.

Table 1 shows the results of the EDX analyses. The chemical compositions found correspond well to the nominal composition and show no significant directionality in the surface planes. The results of the EDX analysis reveal a broader scatter especially in the content of Zr at the free surface. However, both the content of Zr and Ti correspond to the nominal compositions within the experimental error of the method used (about 0.2 wt.%) and the chemical composition seems to be reasonably homogeneous.

WDA point analyses were performed on transversal sections in series along lines going through the regions of a different ribbon thickness parallel to the ribbon plane. No statistically significant differences in the chemical composition were found. Further series of point analyses were performed along lines perpendicular to the ribbon plane in order to detect a possible gradient in the chemical composition. Most of the measurements showed no compositional gradient within the experimental error of the measuring methods. In some cases a slightly higher content of Zr and Ti (about 0.2 wt.%) was found near the free surface. The minimum effective area of the point analysis of several μm^2 did not allow to detect any second-phase particles the sizes of which were expected to be much smaller.

3.2 Phase composition

The SAXS curves measured in all materials are given in Fig. 2. The mean square fluctuation of the scattering density $\overline{(\Delta\rho)^2}$ was calculated from the integrated scattering density as [14]

$$\overline{(\Delta\rho)^2} = \frac{K}{4\pi^2} \int_0^\infty \frac{\mathrm{d}\tilde{\Sigma}}{\mathrm{d}\Omega}(q) \cdot q \cdot \mathrm{d}q, \tag{1}$$

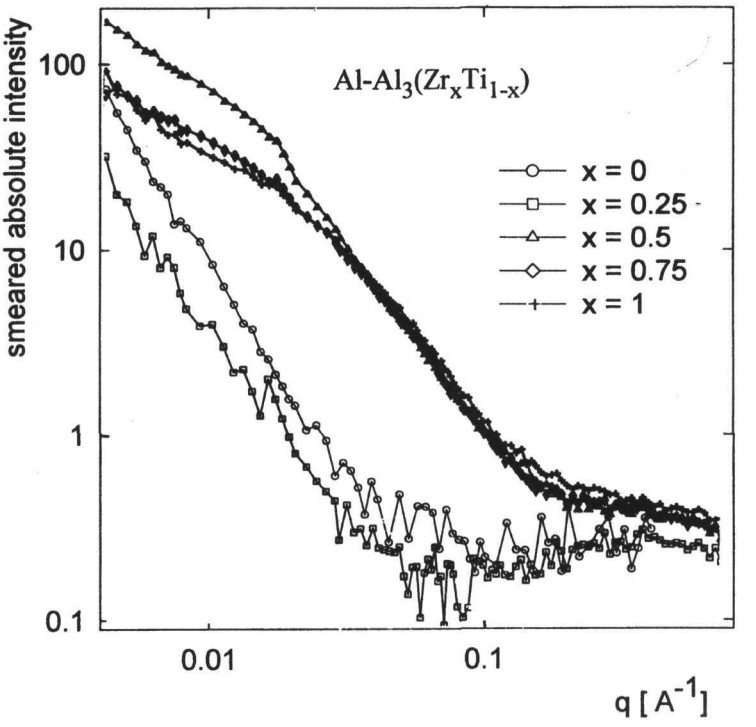

Fig. 2. SAXS curves in the as-melt-spun Al-Zr-Ti alloys.

where $d\tilde{\Sigma}/d\Omega$ is the normalised intensity measured with an infinitely long primary beam (smeared intensity), q is the scattering vector, and K is an instrument constant. This procedure may be applied only in Zr-rich alloys ($x \geq 0.5$) where the scattering curves can be extrapolated to zero scattering vectors with a reasonable accuracy. Nevertheless, even in these alloys the experimental error of $\overline{(\Delta\rho)^2}$ is about 20%.

A two-phase model was adopted in order to deduce some quantitative structural data from SAXS curves. According to this model, the mean square fluctuation of scattering density can be then written as

$$\overline{(\Delta\rho)^2} = \nu_1 \cdot \nu_2 \cdot (\rho_1 - \rho_2)^2, \tag{2}$$

where ν_i and ρ_i $(i = 1, 2)$ are the volume fractions and scattering densities of the matrix and the second-phase particles, respectively. It is considered that the $Al_3(Zr_xTi_{1-x})$ phase forms the second-phase particles. Table 2 shows the com-

Table 2. Results of SAXS measurements

x	$\overline{(\Delta\rho)^2}_{exp}$ 10^{20} cm^{-4}	$\overline{(\Delta\rho)^2}_{th}$ 10^{20} cm^{-4}	ν_2 [%]	D [nm]
1	1.5	5.6	1.4	6
0.75	1.4	4.4	1.6	6
0.5	1.8	3.3	2.8	8
0.25	–	2.3	–	460
0	–	1.4	–	120

parison of experimental values $\overline{(\Delta\rho)^2}_{exp}$ with theoretical ones calculated on the assumption of the phase equilibrium characterised by negligible solid solubilities of Zr and Ti in the Al-matrix and, therefore, by the presence of 5 vol.% of the $Al_3(Zr_xTi_{1-x})$ particles. A big difference between experimental and theoretical values of $\overline{(\Delta\rho)^2}$ shows that the alloys are far from equilibrium and the volume fraction ν_2 of second-phase particles seems to be close to 2%.

Scattering behaviour at high scattering vectors can be described by a modified Porod's law [15]

$$\frac{d\tilde{\Sigma}}{d\Omega}(q) = A + \frac{C_3}{q^3}. \tag{3}$$

Assuming the simplest model of spherical second-phase particles, their diameter D can be evaluated by the following equation:

$$D = \frac{6 \cdot \nu_2}{K \cdot C_3}\pi^2(\rho_1 - \rho_2)^2, \tag{4}$$

where

$$C_3 = \lim_{q\to\infty} q^3 \left(\frac{d\tilde{\Sigma}}{d\Omega}(q) - A\right). \tag{5}$$

Table 2 shows that the characteristic size of second-phase particles in Zr-rich alloys is of several nanometers. The size of particles in Ti-rich alloys cannot be determined as the volume fraction ν_2 of these particles is not known. However, supposing a low hypothetical value of $\nu_2 = 1\%$ the resulting characteristic size of second-phase particles seems to be much bigger than in Zr-rich alloys.

The X-ray diffraction analysis represents an alternative method for the investigation of the phase composition. However, there are two reasons which make this analysis rather difficult in the Al-Zr-Ti alloys studied. The expected volume fraction of non-matrix phases and, therefore, the intensity of their diffraction peaks, is low in the rapidly solidified materials. Additionally, the structure of these phases is very similar to that of pure Al and their most intensive diffraction peaks are

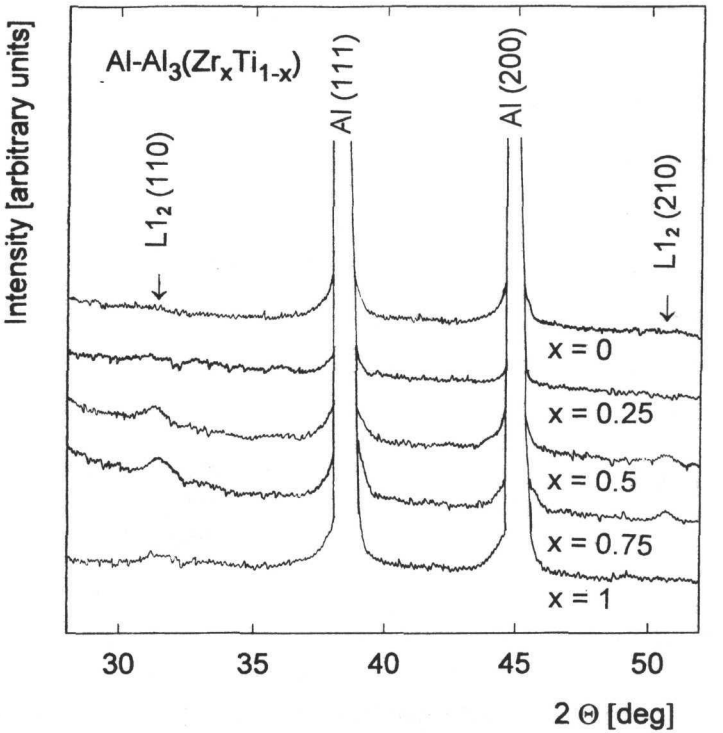

Fig. 3. X-ray diffractograms of the as-melt-spun ribbons.

overlapped by matrix peaks. The presence of these phases may be then proved only by the detection of some less intensive diffraction extra peaks resulting from the ordering of these phases. One may see in Fig. 3 the Al-based matrix peaks and only very small peaks in the Zr-containing alloys at positions corresponding to the (110) and (210) reflections of the metastable $Al_3(Zr_xTi_{1-x})$ phase with the cubic $L1_2$ structure. No extra peaks were found in the Al-Ti alloy. The extra peaks observed in the Zr-containing alloys are very diffuse. Their half-width is about 0.4° so that the lattice parameter may be estimated with the accuracy not better than ± 0.001 nm. Table 3 shows an increase of the lattice parameter of the $Al_3(Zr_xTi_{1-x})$ phase with increasing Zr content. Fig. 4 documents a good correspondence between the lattice parameters measured and the literature data obtained by interpolation from the lattice parameters of both metastable binary Al_3Zr and Al_3Ti alloys [2] under the assumption of the validity of Vegard's law.

As the Zr and Ti atoms dissolved in the Al-matrix modify its lattice parameter,

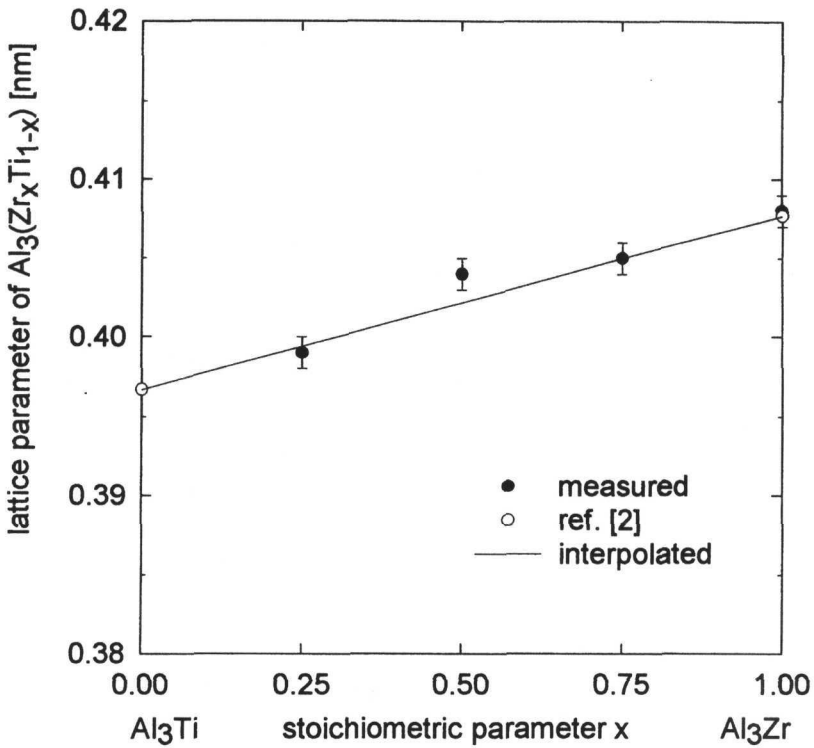

Fig. 4. Dependence of the lattice parameter of the metastable $Al_3(Zr_xTi_{1-x})$ phase on the stoichiometric parameter x.

Table 3. Lattice parameters of phases present in the as-melt-spun Al-Zr-Ti ribbons

x	a (matrix) [nm]	a ($Al_3(Zr_xTi_{1-x})$) [nm]
1	0.4049 ± 0.0004	0.408 ± 0.001
0.75	0.4049 ± 0.0004	0.405 ± 0.001
0.5	0.4051 ± 0.0004	0.404 ± 0.001
0.25	0.4045 ± 0.0004	0.399 ± 0.001
0	0.4042 ± 0.0004	–

the precise measurement of the lattice parameter of the Al-based matrix should enable to estimate its chemical composition. The measured values are summarised in Table 3. A nearly constant lattice parameter of the matrix was observed in the Zr-rich alloys and a slight decrease exceeding the experimental error was found in

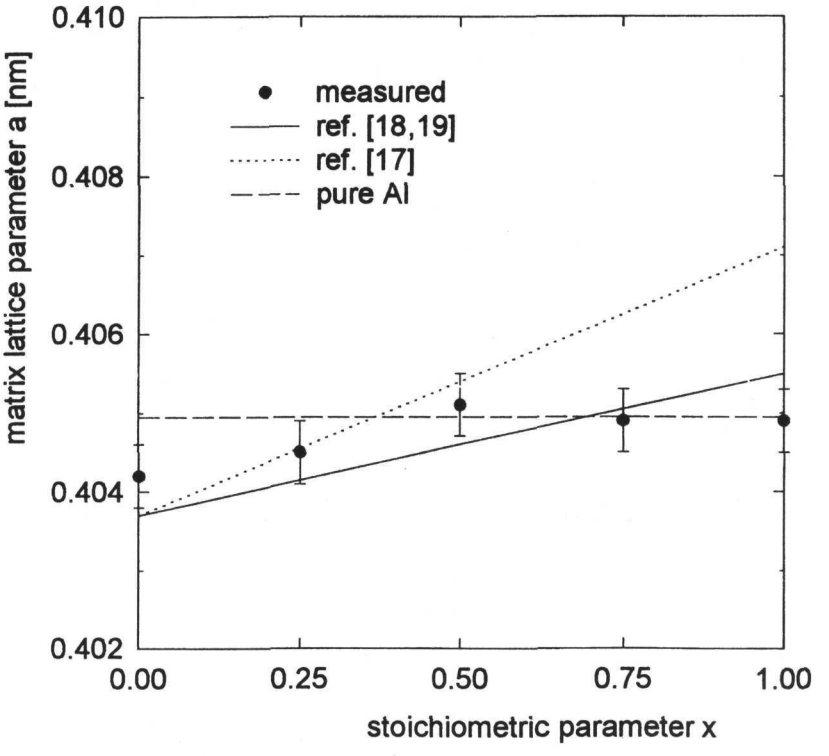

Fig. 5. Dependence of the matrix lattice parameter on the stoichiometric parameter x.

the Ti-rich alloys. The measured values may be compared with the values deduced from literature data. Two hypothetical states are considered:

a) The formation of any second phase in the Al-Zr-Ti alloys studied is completely suppressed due to rapid solidification and all Zr and Ti atoms are dissolved in the matrix.

b) The amounts of Zr and Ti atoms dissolved in the matrix correspond to the equilibrium solid solubility limits.

It was reported that Ti atoms reduce the lattice parameter of the Al-based matrix by −0.00105 nm/at.% [16] while Zr atoms extend it. However, the data from different references are diverse (0.00168 nm/at.% [17] or 0.0004 nm/at.% [18, 19]). The matrix lattice parameters computed for the case a) according to both sets of literature data are plotted in Fig. 5. Equilibrium solid solubilities are about 0.01 wt.% Zr and 0.025 wt.% Ti at room temperature [4]. Such small amounts of solute atoms cannot influence the lattice parameter of the Al-matrix and, therefore,

the lattice parameter of pure Al can be used as the matrix lattice parameter for the case b). It can be seen from Fig. 5 that the measured values of matrix lattice parameter do not simply agree with any of both models.

4. Discussion

The melt-spinning method results usually in remarkable structure inhomogeneities as the solidification rates are significantly different in different parts of the ribbons. The results of the EDX and WDA analyses confirmed that despite of this expected inhomogeneity the chemical composition across the ribbons was reasonably homogeneous without any directionality. This is very important for the interpretation of other results, especially of the microhardness measurements (see part 2).

Rapid solidification with the expected cooling rate of the order of 10^6 K.s^{-1} can extend the solid solubility of Zr and Ti in Al in a significant manner and suppress the formation of second-phase particles. However, the reported data on the extended solid solubility limit and on the presence of second-phase particles in Al-Zr and Al-Ti alloys are very diverse. The explanation of this diversity can be sought not only in the differences in the composition and solidification rates used in individual experiments but also in the selection of experimental methods. For example, transmission electron microscopy yields only local information on the structure and, in case of inhomogeneous structures, the results may be misleading. On the other hand, a general information on the phase composition can be obtained using X-ray diffraction analysis. However, the volume fractions of second phases and the intensities of their diffraction peaks are very low. Also the changes in the lattice parameter of the Al-based matrix due to dissolved Zr and Ti usually lie within the experimental error. In order to avoid this difficulty and to get the more reliable information on the phase composition of the Al-Zr-Ti alloys studied, several experimental methods were combined.

SAXS measurements revealed unambiguously the presence of some sites contributing to the scattered intensity. Assuming that these centres are particles of the $Al_3(Zr_xTi_{1-x})$ phase, their volume fractions and mean sizes were estimated. The volume fraction close to 2% in Zr-rich alloys corresponds only to a very rough estimate. However, it can be concluded that the volume fraction of the second phase is deeply below the value corresponding to the phase equilibrium. Despite of many simplifications (a two phase model, the spherical form of particles) the SAXS results suggest clearly a different size of second-phase particles in Zr-rich and Ti-rich alloys.

The experimental error of the matrix lattice parameter was estimated to be about ± 0.0004 nm. This scatter, together with the ambiguity of data on the influence of dissolved Zr atoms on the lattice parameter of Al, prevents to draw any reasonable conclusion on the phase composition of the Zr-rich alloys. The

decrease in the matrix lattice parameter in the Ti-rich alloys ($x \leq 0.25$) correlates well with the expectation that rapid solidification extends the solid solubility of Ti in Al.

The X-ray diffraction experiments enabled to identify the particle forming phase in the Zr-containing alloys. The extra diffraction peaks observed were interpreted as (110) and (210) reflections of the metastable $Al_3(Zr,Ti)$ phase with the $L1_2$ structure. The decrease in the lattice parameter of this phase with increasing Ti-content (see Table 3) supports the idea that Ti atoms substitute for Zr atoms in the Al_3Zr phase. The measured values of the lattice parameter agree well with the values calculated using the Vegard's law from lattice parameters of both Al-Zr and Al-Ti binary alloys. This suggests that the composition of the $Al_3(Zr_xTi_{1-x})$ corresponds well to the nominal composition.

5. Conclusions

1. The chemical compositions of the Al-Zr-Ti ribbons agree well with the nominal compositions of alloys and no significant composition gradients were observed.

2. The as-melt spun Al-Zr-Ti alloys are not single-phase materials. The SAXS measurement revealed scattering sites of the size below 10 nm in the Zr-rich ($x \geq 0.5$) alloys and much coarser centres of the size above 100 nm in the Ti-rich ($x \leq 0.25$) alloys. The volume fraction of the presumed second phase was estimated to be close to 2 vol.% in the Zr-rich alloys.

3. The presence of the second phase in the as-melt-spun Al-Zr-Ti alloys was confirmed by the X-ray diffraction experiments. The second phase present in the Zr-rich alloys was identified to be the metastable $Al_3(Zr_xTi_{1-x})$ phase. The second phase present in the Ti-rich alloys was not identified.

Acknowledgements

The authors are grateful to Dr. D. Plischke, Crystal Laboratory Göttingen, Germany, for the preparation of thin ribbons. The research was supported by the Grant Agency of the Charles University through the grant No. 283, by the Grant Agency of the Czech Republic through the grant No. 93-2432 and through the fellowship awarded by the Alexander von Humboldt foundation.

REFERENCES

[1] LIFSHITZ, I. M.—SLYOZOV, V. V.: J. Phys. Chem. Solids, *19*, 1961, p. 35.
[2] WAGNER, C.: Z. Elektrochem., *65*, 1961, p. 581.
[3] JONES, H.: Aluminium, *54*, 1978, p. 274.
[4] MONDOLFO, L. F.: Aluminium Alloys: Structure and Properties. London, Butterworth 1976.
[5] DAS, S. K.—DAVIS, L. A.: Mater. Sci. Eng., *98*, 1988, p. 1.
[6] SRINIVASAN, S.—DESCH, P. B.—SCHWARTZ, R. B.: Scripta Metall., *25*, 1991, p. 2513.

[7] NES, E.: Acta Metall., *20*, 1972, p. 499.
[8] ZEDALIS, M.—FINE, M. E.: Scripta Metall., *17*, 1983, p. 1247.
[9] ZEDALIS, M.—FINE, M. E.: Met. Trans. A, *17*, 1986, p. 2187.
[10] CHEN, Y. C.—FINE, M. E.—WEERTMAN, J. R.—LEWIS, R. E.: Scripta Metall., *21*, 1987, p. 1003.
[11] LEWIS, R. E.—CROOKS, D. D.—CHEN, Y. C.—FINE, M. E.—WEERTMAN, J. R.: High temperature Al-Zr-V alloys using rapid solidification processing. In: Proc. 3rd Int. Conf. on Creep and Fracture of Engineering Materials. Eds.: Wilshire, B., Evans, R. W. London, Inst. of Metals 1987, p. 331.
[12] PARAMESWARAN, V. R.—WEERTMAN, J. R.—FINE, M. E.: Scripta Metall., *23*, 1989, p. 147.
[13] JONES, H.: Rapid Solidification of Metals and Alloys. London, Inst. of Metallurgists 1982.
[14] KRATKY, O.: Prog. Biophys., *13*, 1963, p. 105.
[15] RULAND, W.: J. Appl. Cryst., *4*, 1971, p. 70.
[16] HETCH, J. E.: Aluminum: Properties and Physical Metallurgy. Metals Park, OH, ASM 1974, p. 29.
[17] CHEN, Y. C.—FINE, M. E.—WEERTMAN, J. R.: Acta Metall. Mater., *38*, 1990, p. 771.
[18] SAHIN, E.—JONES, H.: Extended solid solubility, grain refinement and age hardening in Al – 1 to 13 wt.% Zr rapidly quenched from the melt. In: Rapidly Quenched Metals III. Ed.: Cantor, B. London, The Metals Soc. 1978, p. 138.
[19] BUROV, L. M.—YAKUNIN, A. A.: Russ. J. Phys. Chem., *42*, 1968, p. 540.

Received: 19.4.1999